August 27-31, 2023
FLORENCE - ITALY
ICWE 16
16th International Conference on Wind Engineering

Estimation of horizontal distributions of short-term visibility reduction by blowing snow based on a meso-scale meteorological simulation

Tsubasa Okaze [1], Risa Kawashima [2], Takeru Ito [3]
Satoshi Omiya [4], Hirofumi Niiya [5], Kouichi Nishimura [6]

[1]*Tokyo Institute of Technology, Yokohama, Japan, okaze.t.aa@m.titech.ac.jp*
[2] *Tokyo Institute of Technology, Yokohama, Japan, kawashima.r.ac@m.titech.ac.jp*
[3] *Tokyo Institute of Technology, Yokohama, Japan, ito.t.by@m.titech.ac.jp*
[4]*Civil Engineering Institute for Cold Region, Sapporo, Japan, somiya@ceri.go.jp*
[5]*Niigata University, Niigata, Niigata, niiya@gs.niigata-u.ac.jp*
[6]*Nagoya University, Nagoya, Nagoya, knishi99@gmail.com*

SUMMARY:
Blowing snow affects human activity in snowy regions. High-density blowing snow, which is enhanced by wind gusts, leads to short-term visibility reduction. This study first conducted field observations in a snowfield in Hokkaido, Japan for two winters. The ratio of the maximum 1-min mean to 10-min mean snow-drift fluxes was analyzed. Then, visibility maps were drawn based on the wind velocity distribution with meso-scale meteorological simulation, the obtained relationships within the observations, and the empirical relationships between snow-drift flux and visibility. The 1-min mean visibility could be decreased to less than half of the 10-min mean visibility.

Keywords: blowing snow, visibility, meso-scale meteorological simulation

1. INTRODUCTION

Blowing snow is wind-driven snow that is falling and/or that has already accumulated but is lifted and blown by strong winds; it often affects human activity in snowy regions. For example, snowdrifts can form within built-up environments. Furthermore, on winter roads, collisions and stuck vehicles often occur owing to poor visibility and snowdrift caused by blowing snow. In addition, wind gusts enhance high-density blowing snow, which leads to short-term visibility reduction. Visibility information is important for road management to prevent such accidents and for drivers to select appropriate routes.

In this study, field observations of blowing snow in a snowfield at Teshikaga, Hokkaido, Japan, were conducted for two winters. Then, the relationship between mean wind velocity and snow-drift flux as well as the snow-drift flux ratio between the 10-min mean and the maximum of the 1-min mean during the 10 min were analyzed. In addition, based on a meso-scale meteorological simulation, the horizontal distributions of wind velocity, snow-drift flux, and visibility were estimated.

2. FIELD OBSERVATION

2.1. Measurement setup

Tower observations for blowing snow were conducted in the winters of 2019 and 2022 in a snowfield in Teshikaga, Hokkaido, Japan. The prevailing wind direction at the observation site was northwest. On the windward side of the observation site, there is no wind obstruction for more than 1 km. Figure 1 shows the installation of the measurement equipment in 2019. Wind velocity and snow-drift flux were measured with an ultrasonic anemometer (Young Company, CYG-81000) and snow particle counter (SPC; Niigata denki, SPC-95 or SPC-S7) at four heights (1.0, 1.5, 3.0, and 7.0 m). Additionally, a back-scatter visibility sensor (Meisei Electric, TZE-4A-HS) was installed at 2.2 m height. In 2022, another back-scatter visibility sensor (IR System, MiniBSV) was installed at 2.2 m. Sampling rates were 10 Hz for wind velocity, 1 Hz for snow-drift flux, 1/600 Hz for visibility by TZE-4A-HS, and 1/60 Hz for visibility by MiniBSV, respectively.

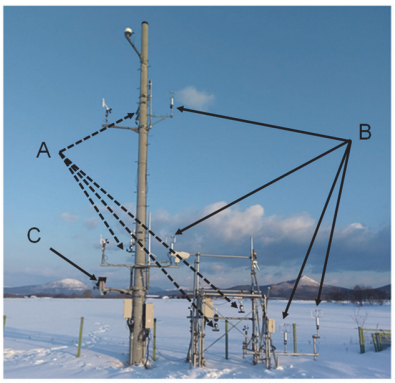

Figure 1. Installation of measurement equipment in 2019. A: SPC, B: ultrasonic anemometer, C: visibility sensor.

2.2. Observation results

According to Takeuchi et al. (1986), the threshold wind speed for the intermittent event of blowing snow was a 10-min mean wind speed of 8.5 m/s at 7.0 m height when the air temperature was less than -2.0 °C. By following these conditions, a total of 2128 10-min periods were extracted as blowing snow events. Note that periods in which the total number of blowing snow particles measured by SPC at 1.0 m height was less than 1000 were removed.

Figure 2 shows the relationship between the 10-min mean wind velocity at 10 m height and the 10-min mean snow-drift flux at 1.0 m. The mean wind velocity at 10 m was calculated from the mean wind velocities observed at the four heights by extrapolation using a logarithmic law. As the wind velocity increased, the snow-drift flux rapidly increased. By applying the least-squares method, the snow-drift flux at 1.0 m, q (g/m^{2}s), was given as a function of mean wind speed at 10 m, U (m/s):

$$q = 1.27 \times 10^{-6} U^{5.88}. \quad (1)$$

Figure 3 shows the relationship between the snow-drift fluxes of the 10-min mean and the maximum of the 1-min mean during the focused 10 min at 1.0 m. The maximum of the 1-min mean varied within a range of 1.5 to 6 times the 10-min mean. The relationship between the 10-min mean wind velocity at a height of 10 m and the ratio of the maximum values of the 1-min

maximum to the 10-min mean of them, R (-), is shown in Figure 4. As the wind velocity increased, the variation decreased, and the ratio converged to a value of approximately three. The least-squares method was applied, and the ratio of snow-drift fluxes was expressed as a function of the mean wind velocity:

$$R = 1.73 \times 10e^{-2.29U} + 1.83. \quad (2)$$

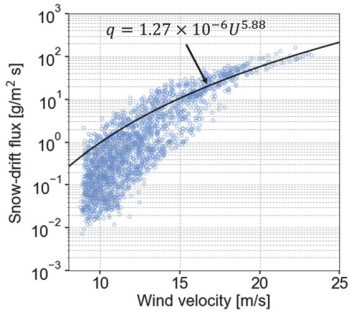

Figure 2. Relationship between 10-min mean wind velocity and snow-drift flux.

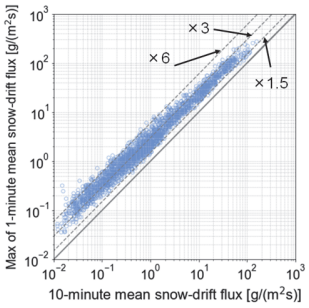

Figure 3. Relationship between 10-min mean and maximum of 1-min snow-drift fluxes.

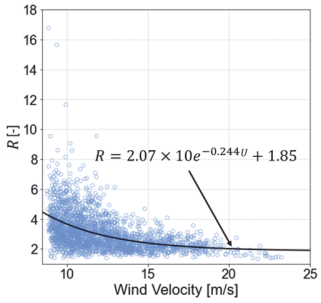

Figure 4. Relationship between 10-min mean wind velocity and snow-drift flux ratio.

3. VISIBIITY MAP BASE ON MESO-SCALE METEOROLOGICAL SIMULATION

3.1. Outline of simulation

A meso-scale meteorological simulation was performed using the regional climate model WRF version 3.7.1. The simulation was conducted from 21:00 on February 19 to 23, 2022, when a strong snowstorm occurred, including the spin-up. A system of four nested domains was used, as shown in Figure 5. The horizontal grid sizes for the domains were 25, 5, 1, and 0.333 km.

3.2. Simulation results

Figure 6 shows a comparison of the wind direction and velocity at 10 m at the observation site. From the dawn of February 21st, the wind speed began to escalate, reaching over 20 m/s by the dawn of February 22nd. Although the simulation results slightly overestimated the wind speed, they effectively captured the variations in both the wind direction and speed compared to the observations. Figure 7a illustrates the distribution of the horizontal wind velocity at 10 m at 00:00 on February 22nd. Owing to the influence of the gap wind, a region of strong wind with velocities ranging from 20 to 24 m/s was locally predicted near the outlet of the valley located near the observation site. To evaluate visibility, the relationship between the snow-drift flux and visibility proposed by Takechi et al. (2009), expressed as eq. (3), was applied as follows:

$$\log(Vis) = -0.886 \log(q) + 2.648, \quad (3)$$

where Vis denotes the visibility (m), and q is snow-drift flux in g/m^{2}s. Figure 7b shows the distribution of the 10-min mean visibility, and Figure 7c shows the distribution of the minimum 1-min mean visibility. The 10-min mean visibility was about less than 20 m, whereas the minimum 1-min mean one was less than 10 m. This tendency corresponded with the measurement from the back-scatter visibility sensor (MiniBSV).

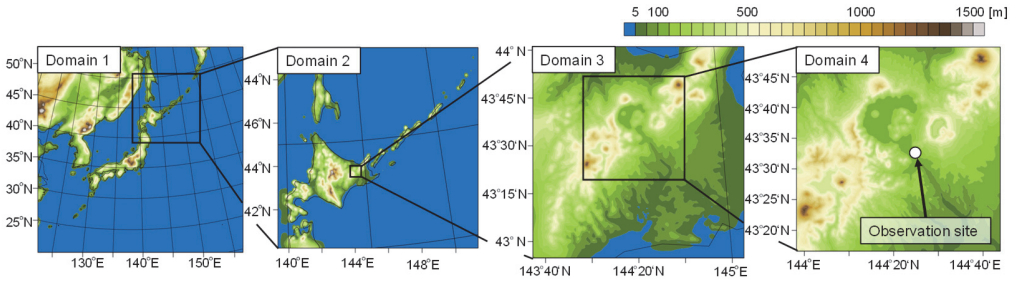

Figure 5. Calculation domains.

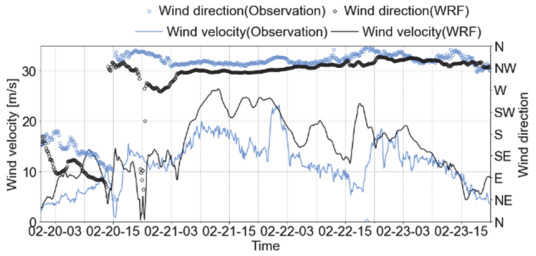

Figure 6. Comparison of wind velocity.

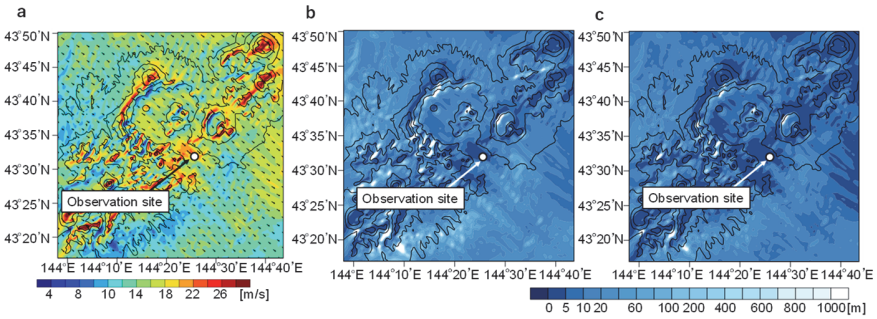

Figure 7. Wind velocity and visibility maps at 00:00 on February 22nd. a: wind velocity at 10 m, b: 10-min mean visibility, c: minimum of 1-min mean visibility.

7. CONCLUSIONS

Field observations were conducted in a snowfield in Hokkaido, Japan. The relationship between 10-min mean wind velocity and mean snow-drift flux was obtained. Then, the ratio of the maximum 1-min mean to 10-min mean snow-drift fluxes was analyzed. Finally, visibility maps were shown based on meso-scale meteorological simulation.

ACKNOWLEDGEMENTS

This work was supported by JSPS KAKENHI (grant numbers 21H01489, 21H04601, and 20H01983).

REFERENCES

Takechi, H. et. al., 2009. Annual Report on Snow and Ice Studies in Hokkaido 28, 17–20.

Takeuchi, M. et al., 1986. The Proceedings of the annual meeting on The Japanese Society of Snow and Ice, 256.